

**Shape-Changing Linear Molecular Bottlebrushes with Dually
pH- and Thermo-Responsive Diblock Copolymer Side Chains**

Journal:	<i>Polymer Chemistry</i>
Manuscript ID	PY-ART-08-2018-001137.R2
Article Type:	Paper
Date Submitted by the Author:	18-Sep-2018
Complete List of Authors:	Kent, Ethan; The University of Tennessee, Department of Chemistry Henn, Daniel; The University of Tennessee, Department of Chemistry Zhao, Bin; The University of Tennessee, Department of Chemistry

Shape-Changing Linear Molecular Bottlebrushes with Dually pH- and Thermo-Responsive Diblock Copolymer Side Chains

*Ethan W. Kent, Daniel M. Henn, and Bin Zhao**

Department of Chemistry, University of Tennessee, Knoxville, Tennessee 37996, United States

* Corresponding author. Email: bzhao@utk.edu

Abstract

This article reports on the synthesis and responsive behavior of shape-changing linear molecular bottlebrushes containing dually pH- and thermo-responsive diblock copolymer side chains. Using a “click” grafting to method, we synthesized linear homografted molecular brushes composed of diblock copolymer side chains with pH-responsive poly(2-(*N,N*-diethylamino)ethyl methacrylate) (PDEAEMA) as inner block and thermoresponsive poly(methoxytri(ethylene glycol) acrylate) (PTEGMA) as outer block. Dynamic light scattering studies showed that the brushes exhibited a sharp decrease in hydrodynamic size with increasing pH across the pK_a of PDEAEMA and the size leveled off at higher pH. This is in contrast to the molecular brushes with only PDEAEMA homopolymer side chains, which underwent aggregation and precipitation in basic solution even at a concentration of 0.2 mg/g. Atomic force microscopy confirmed the cylindrical morphology of the brushes at acidic pH and pH-induced cylinder-to-globule transitions. In addition, the use of PTEGMA as outer block provided another means to control the solution state of the collapsed brushes; above the lower critical transition temperature of PTEGMA, the brushes clustered at higher concentrations but remained unaggregated at lower concentrations. The switching of molecular shape, stabilization of collapsed nano-objects, and control of solution state reported here may enable new potential applications of stimuli-responsive shape-changing molecular brushes.

Introduction

Molecular bottlebrushes, a type of graft copolymers in which polymeric side chains are densely tethered to a backbone polymer,¹⁻³ have received growing interest in recent years because of their intriguing properties and great potential in a wide variety of applications such as photonic crystals,⁴ lubrication,⁵ and supersoft elastomers.⁶ In good solvents, linear macromolecular brushes adopt cylindrical or worm-like conformations, a result of strong excluded volume interactions between side chains.¹⁻³ The dimensions are determined by the aspect ratio of backbone to side chain length, grafting density, and solvent quality. These macromolecules are commonly synthesized by one or a combination of two of the following three methods: (i) grafting-through, in which macromonomers are polymerized directly into brushes (e.g., by using the Grubbs catalyst),^{1-4,7-9} (ii) grafting-from, in which side chains are grown from pendant initiation sites on a polymer backbone,^{1-3,10-19} and (iii) grafting-to, in which end-functionalized side chain polymers are covalently attached to a backbone polymer.¹⁷⁻²² Each method has advantages and drawbacks. For example, the grafting-to method provides the advantages of allowing for thorough characterization of backbone and side chain polymers and modular synthesis of brush polymers via simultaneous grafting of different side chain polymers onto the same backbone. However, the grafting density of the brushes tends to be low. In the past decade, the copper-catalyzed azide-alkyne cycloaddition (CuAAC) reaction²³ has emerged as a powerful and versatile means for preparing molecular bottlebrushes with high grafting densities via grafting-to.¹⁷⁻²⁶

Stimuli-responsive molecular brushes,²⁴⁻⁴¹ composed of side chain polymers that can undergo large and abrupt conformational changes in response to external stimuli, are of great interest to fundamental study of the behavior of stimuli-responsive polymers and to potential technological uses. Many of these brushes have been shown to exhibit intriguing worm-to-globule shape

transitions or vice versa upon application of external stimuli. For example, Schmidt et al. synthesized thermoresponsive poly(*N*-isopropylacrylamide) (PNIPAM) molecular brushes by a “grafting-from” method using atom transfer radical polymerization (ATRP) and observed by atomic force microscopy (AFM) that these brushes underwent a worm-to-sphere shape change when the temperature was raised to above the LCST of PNIPAM.³⁰ The unimolecular spherical nano-objects, however, were unstable; they aggregated and eventually precipitated out of the solution. Using a similar approach, Matyjaszewski et al. prepared loosely grafted poly(acrylic acid) molecular brushes and studied their conformations on mica at different pH values by AFM.³¹ The brushes underwent a globule-to-extended conformational transition when the pH was changed from acidic to basic. Müller et al. synthesized poly(*N,N*-dimethylaminoethyl methacrylate) (PDMAEMA) molecular brushes; cryo-transmission electron microscopy showed that the brushes were worm-like at pH = 7 but strongly contracted at pH = 10.³² They also reported the conformational switching of cationic quaternized PDMAEMA brushes via the formation of ionic and supramolecular inclusion complexes in dilute conditions.³⁴ Using a Langmuir-Blodgett trough, Sheiko et al. demonstrated reversible worm-to-sphere shape transitions of cylindrical poly(*n*-butyl acrylate) molecular brushes by lateral compression at the water-air interface.^{35,36}

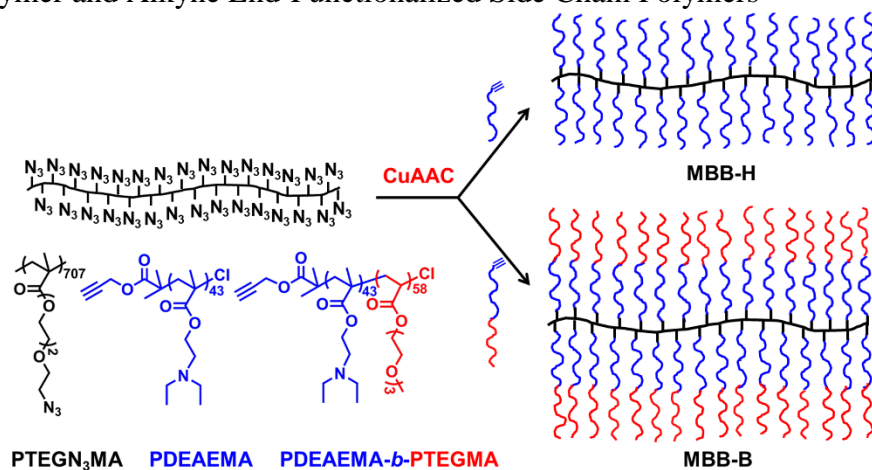
While intriguing, the worm-to-globule shape changes of molecular brushes have been restricted to dilute solutions, typically <1.0 mg/g, or at liquid or solid-air interfaces,^{24-27,30,34,37-39} which has greatly limited the possible uses of shape-changing molecular bottlebrushes in potential applications, such as molecular actuators, delivery of substances, biomimetic catalysis, etc. We recently reported the synthesis and shape changing study of linear binary heterografted molecular brushes composed of a thermoresponsive polymer and a hydrophilic poly(ethylene oxide) (PEO) as side chains and showed that the collapsed thermoresponsive side chains were stabilized by PEO

in water.²⁴ While a 1.0 mg/g aqueous solution of the corresponding thermoresponsive homopolymer brushes turned cloudy upon heating above the LCST, the binary heterografted molecular brushes underwent unimolecular worm-to-globule transitions and the solution stayed clear at the same concentration. The shape changing of these brushes was utilized to regulate the interaction of brush molecules with avidin in the environment by hiding and exposing biotin functional groups that were incorporated into the thermoresponsive side chains. We further discovered that the worm-to-globule shape transitions of binary heterografted molecular brushes can be achieved in moderately concentrated aqueous solutions if the PEO is significantly longer so that the thermoresponsive side chains are well shielded by PEO to avoid intermolecular association during the LCST transition.²⁶

Besides the binary heterografted molecular brushes for achieving worm-to-stabilized globule shape transitions, it is also possible to use homografted molecular brushes with a stimuli-responsive diblock copolymer as side chains (i.e., core-shell brushes¹⁻³), in which the inner block is a stimuli-responsive polymer whose solubility change, triggered by environmental stimuli, drives the shape transition of the brushes from worm-like to globular and the outer block serves as a stabilizer. In addition, if the outer block is also stimuli-responsive, the state of the brushes in water can be controlled by a second stimulus. To test this hypothesis, we synthesized in the present work linear homografted molecular brushes composed of poly(2-(*N,N*-diethylamino)ethyl methacrylate)-*b*-poly(methoxytri(ethylene glycol) acrylate) (PDEAEMA-*b*-PTEGMA) side chains (MBB-B), where PDEAEMA is the inner block, by a “grafting to” method using CuAAC (Scheme 1). PDEAEMA is a pH-responsive polymer with a pK_a of 7.4 in water,^{42,43} while PTEGMA is a thermoresponsive polymer with a LCST of 58 °C.⁴⁴⁻⁴⁶ We chose PDEAEMA as the inner block because this polymer exhibits a solubility transition in water from very hydrophilic at low pH to

very hydrophobic at high pH, providing a strong driving force for the worm-to-globule shape transition. For comparison, we also made a molecular brush composed of only PDEAEMA side chains (MBB-H). We showed that MBB-B underwent a cylinder-to-globule shape transition with increasing pH from acidic to basic at room temperature and the collapsed globular state was stabilized by the outer block. In contrast, MBB-H precipitated out from the solution when the pH was increased to near the pK_a of PDEAEMA. We further demonstrated the ability to control the solution state of MBB-B in water by varying the temperature.

Scheme 1. Synthesis of Stimuli-Responsive Molecular Bottlebrushes MBB-B and MBB-H via Copper-Catalyzed Azide-Alkyne Cycloaddition (CuAAC) Click Reaction between Azide-Bearing Backbone Polymer and Alkyne End-Functionalized Side Chain Polymers



Experimental Section

Materials. CuCl (99%, Acros) was purified by stirring in glacial acetic acid overnight; the solids were collected by vacuum filtration, thoroughly washed with absolute ethanol and diethyl ether, and then dried under high vacuum. 2-(*N,N*-Diethylamino)ethyl methacrylate (DEAEMA, 98.5%, TCI), ethyl 2-bromoisobutyrate (EBiB, 98%, Aldrich), and *N,N,N',N'',N'''*-pentamethyl-diethylenetriamine (PMDETA, 99%, Acros) were purified by vacuum distillation over calcium

hydride. The azide-bearing backbone polymer, PTEGN₃MA (Scheme 1), with a degree of polymerization (DP) of 707, was synthesized via a procedure reported previously (Scheme S1),²⁴ and the characterization data are included in Figures S1. Triethylene glycol monomethyl ether (97%, Aldrich), 1,1,4,7,10,10-hexamethyltriethylenetetramine (HMTETA, 97%, Aldrich), and triethylamine (99%, Alfa Aesar) were used as received. Methoxytri(ethylene glycol) acrylate (TEGMA) was synthesized by the reaction of tri(ethylene glycol) monomethyl ether and acryloyl chloride,^{44,45} and the molecular structure was confirmed by ¹H NMR spectroscopy analysis. Propargyl 2-bromoisobutyrate (PBiB) was synthesized according to a procedure described before.²⁴ All other chemicals were purchased from either Aldrich or Fisher and used as received.

General Characterization. The molecular weights and dispersities of the backbone polymer PTEGN₃MA and molecular bottlebrushes with diblock copolymer side chains were determined by size exclusion chromatography (SEC), performed at 50 °C using a PL-GPC 50 Plus system (an integrated GPC/SEC system from Polymer Laboratories, Inc.) with a differential refractive index detector, one PLgel 10 μm guard column (50 × 7.5 mm, Agilent Technologies), and three PLgel 10 μm mixed-B columns (each 300 × 7.5 mm, linear range of molecular weight from 500 to 10,000,000 Da, Agilent Technologies). *N,N*-Dimethylformamide (DMF) containing 50 mM LiBr was used as the carrier solvent at a flow rate of 1.0 mL/min for analysis. SEC of alkyne end-functionalized PDEAEMA and PDEAEMA-*b*-PTEGMA side chain polymers was performed at ambient temperature using a PL-GPC 20 (an integrated GPC/SEC system from Polymer Laboratories, Inc.) with a refractive index detector, one PLgel 5 μm guard column (50 × 7.5 mm, Agilent Technologies), and two PLgel 5 μm mixed-C columns (each 300 × 7.5 mm, linear range of molecular weights from 200 to 2,000,000 Da, Agilent Technologies). THF was used as the eluent at a flow rate of 1.0 mL/min. Each SEC system was calibrated with a set of narrow disperse

linear polystyrene standards (Scientific Polymer Products, Inc.). ^1H NMR spectra were recorded on a Varian VNMRS 500 NMR spectrometer, using residual solvent proton signal as the internal standard.

ATRP Synthesis of PDEAEMA and PDEAEMA-*b*-PTEGMA. PBiB (112.8 mg, 0.550 mmol), DEAEMA (8.157 g, 44.03 mmol), CuCl (55.1 mg, 0.557 mmol), HMTETA (161.1 mg, 0.699 mmol), and anisole (12.041 g) were added to a 50 mL two-necked round bottom flask and degassed by three freeze-pump-thaw cycles. After the polymerization proceeded at 50 °C for 2.25 h, the reaction mixture was opened to air and passed through a neutral alumina (top)/silica gel (bottom) column with methylene chloride (200 mL). The volatiles were removed by rotary evaporation. The concentrated residue was diluted with THF (15 mL) and then precipitated in hexanes (150 mL) in a dry ice/acetone bath three times. The polymer was dissolved in THF and transferred to a round bottom flask, concentrated by rotary evaporation, and dried under high vacuum (3.353 g). SEC analysis results (Figure S2): $M_{n,SEC} = 6500$ Da and PDI = 1.17, relative to polystyrene standards. The DP of PDEAEMA was 43, calculated from the monomer-to-initiator molar ratio and the monomer conversion (53.7%), determined by ^1H NMR analysis of the ester ($-\text{COOCH}_2-$) peaks from the monomer (4.17-4.29 ppm) and the polymer (3.95-4.16 ppm).

PDEAEMA (DP = 43, 1.007 g, 0.124 mmol), TEGMA (3.400 g, 15.58 mmol), CuCl (12.8 mg, 0.129 mmol), PMDETA (27.9 mg, 0.161 mmol), and anisole (5.034 g) were added to a 25 mL two-necked round bottom flask. The reaction mixture was degassed via three freeze-pump-thaw cycles before the flask was placed in a 100 °C oil bath. After 24 h, the polymerization was stopped, and the mixture was diluted with THF and then passed through a basic alumina (top)/silica gel (bottom) column to remove the copper catalyst. The solvents were evaporated using a rotavapor; the concentrated residue was dissolved in THF (10 mL) and precipitated in hexanes (100 mL) in

an ice/water bath four times. The polymer was collected and dried under high vacuum (0.977 g). SEC analysis (Figure S2): $M_{n,SEC} = 14.1$ kDa, and PDI = 1.21, relative to polystyrene standards.

Synthesis of Linear Homografted Molecular Bottlebrushes with PDEAEMA-*b*-PTEGMA Side Chains (MBB-B). PTEGN₃MA (0.226 g of a 14.30 mg/g stock solution in THF, 3.23 mg, 0.0133 mmol) and PDEAEMA-*b*-PTEGMA (6.489 g of a 76.61 mg/g stock solution in THF, 497.1 mg, 0.0239 mmol) were added to a vial equipped with a magnetic stir bar; a portion of THF (3.324 g) was evaporated under N₂ stream to concentrate the mixture. CuCl (1.5 mg, 0.015 mmol) was then added, and the vial was sealed with a rubber septum; the headspace was purged with nitrogen for 15 min using needles, followed by the injection of PMDETA (5.0 μ L, 0.024 mmol) and purging with nitrogen for additional 15 min. After the reaction proceeded at room temperature for 22 h, benzyl 2-propynyl ether (30 μ L) was injected via a microsyringe to cap unreacted azide moieties. The reaction mixture was stirred at ambient temperature for an additional 3 h and then passed through a silica gel (bottom)/basic alumina (top) column to remove copper catalyst using THF as eluent. The brushes were concentrated and purified by fractionation using THF (2 mL) and hexanes (5 mL) four times to remove the unreacted side chain polymer. The purified brush polymer MBB-B was dried under high vacuum (yield: 156.8 mg) and stored in THF with a concentration of 10.20 mg/g in a freezer. The grafting density of MBB-B was determined to be 75.0 % from the analysis of SEC peak areas of the brushes (42.03%) and the side chain polymer (57.97%) in the final reaction mixture. SEC results: $M_{n,SEC} = 1,783$ kDa and $D = 1.13$, relative to polystyrene calibration.

Synthesis of Molecular Bottlebrushes with PDEAEMA Side Chains (MBB-H). PTEGN₃MA (0.351 g of a 14.30 mg/g stock solution in THF, 5.02 mg, 0.0206 mmol) and PDEAEMA (0.940 g of a 0.294 g/g stock solution in THF, 276 mg, 0.0341 mmol) were added to

a vial along with THF (3.896 g) and magnetic stir bar. While stirring, CuCl (2.1 mg, 0.021 mmol) was added, and the vial was sealed with a rubber septum, and then the headspace was purged with nitrogen through needles for 15 min. PMDETA (5.0 μ L, 0.024 mmol) was injected and the headspace was purged for an additional 15 min before the needles were removed. After 24 h, a sample was taken from the reaction mixture, and benzyl 2-propynyl ether (50 μ L) was injected to cap unreacted azide groups. After 3 h, the vial was opened to air, and the solution was diluted with CH₂Cl₂ (50 mL) and passed through a neutral alumina (top)/silica gel (bottom) column with additional CH₂Cl₂ (100 mL). The brush solution was concentrated by rotary evaporation, and the brushes were purified by fractionation in a mixture of THF and hexanes (1 : 10, v/v) in an ice/water bath to remove the unreacted side chains. The purified brushes were dried under high vacuum to yield a slightly yellow, rubbery polymer (120.1 mg, 69.6% yield). The grafting density was 82.0%, determined from the conversion of alkyne end group (CH \equiv CCH₂-, 4.62 ppm) relative to the ester CH₂ in the polymers (-COOCH₂-, 4.10-3.90 ppm) (Figure S4A). The removal of free side chains was verified by ¹H NMR analysis that showed the disappearance of alkyne end group (Figure S4B), and the brushes were confirmed by atomic force microscopy, which revealed worm-like MBB-H molecules spin cast on bare mica from an acidic solution (Figure S5).

Dynamic Light Scattering (DLS) Study of Molecular Bottlebrushes MBB-B and -H in Water. DLS was performed using a Malvern Zetasizer Nano ZS instrument equipped with a He-Ne 633 nm laser and a temperature controller at a scattering angle of 173°. For each brush sample, a 5.0 mg/g solution was prepared by dissolving the brushes in a 10 mM KH₂PO₄ buffer solution, adjusting the pH to 5.00 with 0.1 M HCl, and stirring at room temperature overnight to ensure complete dissolution. More dilute solutions (1.0, 0.5 or 0.2 mg/g) were prepared by diluting a portion of the 5.0 mg/g solution with a 10 mM buffer solution with pH of 5.00. The pH of the

solution was gradually adjusted using 0.1 M NaOH and 0.1 M HCl, monitored by an Accumet AB15 pH meter (calibrated with pH = 4.01, 7.00, and 10.01 standard buffer solutions), and allowed to equilibrate for 15 min. A portion of the solution was then transferred into a DLS tube without filtering and loaded into the DLS instrument; the temperature was set at 25 °C, and the measurements were taken after equilibration for 10 min. For MBB-B with a concentration of 1.0 mg/g at pH = 8.50, a temperature ramp was performed from 20 to 65 °C, with 5 min of equilibration at each selected temperature. Each reported DLS value was an average of 3 measurements, each of which was comprised of 10 runs. In this work, z-average hydrodynamic diameters were used.

Atomic Force Microscopy (AFM) Study of Molecular Bottlebrushes. AFM study of MBB-B and -H molecular brushes was performed using a Digital Instruments Multimode IIIa Scanning Probe Microscope in tapping mode under ambient conditions. Reflective Al-coated Si probes (Budget Sensors) with a nominal resonant frequency of 300 kHz and a force constant of 40 N/m were employed. PMMA coated mica substrates were prepared by cleaving a clean layer of mica disk (Ted Pella, Inc.) with a single-sided Scotch tape, placing three drops of a 1 wt% solution of PMMA ($M_n = 54.9$ kDa) in CHCl_3 onto the disk, and spinning the solution off at 3000 rpm to create a thin film. Aqueous solutions of molecular brushes with concentrations ranging from 0.01 to 0.1 mg/g in 2.5 mM phosphate buffer were prepared by dilution of brush solutions with higher concentrations and spin cast onto the PMMA-coated mica at 3000 rpm. The solution pH was measured with a pH meter and adjusted to a desired value using 0.1 M NaOH and 0.1 M HCl solutions prior to spin casting. When an elevated temperature was used, the spin casting stage was heated to that temperature along with the mica disk prior to the spin casting process.

Results and Discussion

Synthesis of Azide-Bearing Backbone Polymer and Side Chain Polymers. Molecular bottlebrushes MBB-B and -H were synthesized by a “grafting-to” method using CuAAC. The azide-functionalized backbone polymer, PTEGN₃MA (Scheme 1), with a degree of polymerization (DP) of 707, a dispersity of 1.10, and degree of azide functionalization > 99%, was prepared by following a previously reported procedure.²⁴ Briefly, an ATRP of tri(ethylene glycol) mono(*t*-butyldimethylsilyl) ether methacrylate was conducted first, followed by a series of post-polymerization reactions to install azide functionality, including the removal of *tert*-butyldimethylsilyl ether protecting groups, tosylation of the resulting hydroxyl moieties, and then substitution of tosylate groups with azide via reaction with sodium azide (Scheme S1). A high DP of 707 for the backbone polymer was used to ensure a high aspect ratio of backbone to side chain length, which is necessary for shape changing.

Alkyne end-functionalized pH-responsive PDEAEMA and dually pH- and thermo-responsive diblock copolymer PDEAEMA-*b*-PTEGMA were made by ATRP. The polymerization of DEAEMA was carried out in anisole using propargyl 2-bromoisobutyrate (PBiB) as initiator and CuCl/HMTETA as the catalyst/ligand in molar ratios of $[M]_0 : [I]_0 : [CuCl] : [HMTETA] = 80 : 1 : 1 : 1.3$. The polymerization was carried at 50 °C and stopped after 2.25 h; SEC analysis showed that the ATRP of DEAEMA was well controlled and the polymer exhibited a single, narrow distribution with a $M_{n,SEC}$ of 6.5 kDa and a PDI of 1.17 (Figure S2). The DP of the obtained PDEAEMA was 43, calculated from the monomer conversion, determined from ¹H NMR analysis by comparing the integrals of the ester (-COOCH₂-) peaks of the monomer (4.17-4.29 ppm) and polymer (3.95-4.16 ppm) in the final reaction mixture, and the monomer-to-initiator molar ratio. The catalyst was removed by passing the mixture through a neutral alumina/silica gel column, and

the polymer was purified by repetitive precipitation from THF into hexanes in a dry ice/acetone bath.

The diblock copolymer, PDEAEMA-*b*-PTEGMA, was synthesized by ATRP of TEGMA from the PDEAEMA macroinitiator in anisole at 100 °C for 24 h using CuCl/PMDETA as catalyst/ligand. The molar ratios of $[M]_0/[I]_0/[CuCl]/[PMDETA] = 126/1/1/1.3$. From SEC analysis, the peak shifted to the higher molecular weight side compared to the macroinitiator and broadened slightly, giving a $M_{n,SEC}$ of 14.1 kDa and PDI of 1.21 (Figure S2). The diblock copolymer was purified by passing of the mixture through a basic alumina/silica gel column and multiple precipitation in hexanes at 0 °C. A DP of 58 for the PTEGMA block was calculated from 1H NMR analysis of the purified, dried polymer by comparing the ester peaks ($-COOCH_2-$) of the PTEGMA block (4.09-4.24 ppm) and the PDEAEMA block (3.89-4.08 ppm) (Figure S3). The characterization data for the azide-functionalized backbone polymer and side chain polymers are summarized in Table 1.

Table 1. Characterization Data for Backbone, Side Chain Polymers, and Molecular Brushes

Polymer Sample	$M_{n,SEC}$ (kDa)	\mathcal{D}	DP	Grafting density
PTEGN ₃ MA	307.1 ^a	1.10 ^a	707 ^c	-
PDEAEMA	6.5 ^b	1.17 ^b	43 ^c	-
PDEAEMA- <i>b</i> -PTEGMA	14.1 ^b	1.21 ^b	43, ^c 58 ^d	-
MBB-B (PDEAEMA- <i>b</i> -PTEGMA side chains)	1783 ^a	1.13 ^a	-	75.0 % ^e
MBB-H (PDEAEMA side chains)	-	-	-	82.0 % ^f

^a The number-average molecular weight ($M_{n,SEC}$) and dispersity (\mathcal{D}) were determined by SEC relative to polystyrene standards using PL-GPC 50 Plus with DMF containing 50 mM LiBr as eluent. ^b Obtained by SEC relative to polystyrene standards using PL-GPC 20 with THF as solvent. ^c Calculated from the monomer-to-initiator ratio and monomer conversion by 1H NMR spectroscopy analysis. ^d Determined by comparing characteristic peaks of the two blocks in the 1H NMR spectrum. ^e The grafting density was determined by using the ratio of SEC peak areas of brushes and unreacted side chains in the final mixture and the feed ratio of backbone to side chains. ^f Determined by 1H NMR spectroscopy analysis of the conversion of alkyne end group of PDEAEMA using the ester $-COOCH_2-$ peak of PDEAEMA as reference.

Synthesis of MBB-B and MBB-H. Linear homografted molecular bottlebrushes, MBB-B with pH- and thermo-responsive PDEAEMA-*b*-PTEGMA side chains and MBB-H with PDEAEMA side chains, were synthesized by a “grafting to” method whereby the corresponding alkyne end-functionalized side chain polymer was “clicked” onto the azide-bearing backbone, PTEGN₃MA, via CuAAC reaction. CuCl/PMDETA were used as the catalyst/ligand system, and the reactions were carried out in THF at ambient temperature. For MBB-B, the feed molar ratio of PTEGN₃MA repeat units to PDEAEMA-*b*-PTEGMA side chains was 1 : 1.79; this high ratio was used to ensure that a high grafting density would be achieved. After 22 h, an excess of propargyl benzyl ether was injected in an attempt to cap the unreacted azide groups. SEC showed a high molecular weight peak (Figure 1A), indicating the formation of brushes; the relative peak areas of the brushes and the unreacted side chains from SEC analysis of the final mixture were 42.03 % and 57.97 %, respectively. Using these values and the feed molar ratio of backbone repeat units to the side chains, the grafting density of MBB-B was calculated to be 75.0%. The reaction mixture was passed through a basic alumina/silica column to remove the copper catalyst and purified by fractionation in a THF/hexanes mixture to remove the unreacted side chains, which was confirmed by SEC analysis (Figure 1A); the $M_{n,SEC}$ and \mathcal{D} of the purified brushes were 1783 kDa and 1.13, respectively, relative to polystyrene standards. Note that the slight shift of the brush peak was likely caused by the loss of some lower molecular weight brush molecules during the fractionation. Figure 1B shows the ¹H NMR spectrum of MBB-B in CDCl₃, which is similar to that of PDEAEMA-*b*-PTEGMA side chain polymer (Figure S3B).

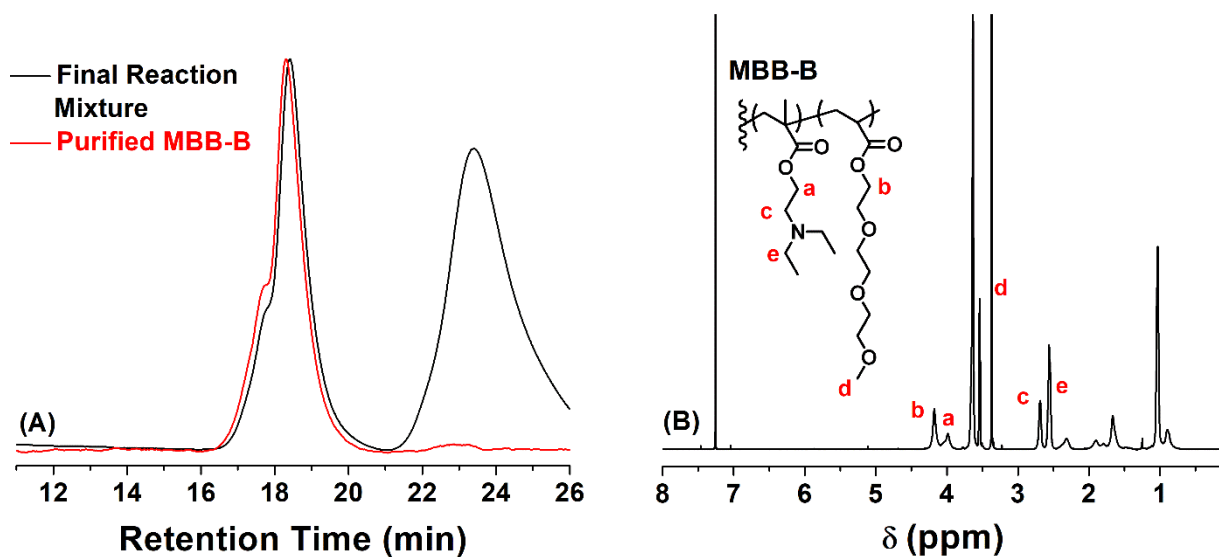


Figure 1. (A) SEC traces of the final reaction mixture and the purified molecular brushes with PDEAEMA-*b*-PTEGMA side chains (MBB-B). (B) ^1H NMR spectrum of the purified MBB-B brushes in CDCl_3 .

For comparison, we also synthesized homografted molecular brushes with pH-responsive homopolymer PDEAEMA side chains (Scheme 1). Similarly, the reaction was carried out in THF with a feed molar ratio of 1 : 1.66 for the backbone repeat units to the side chain polymer. However, the characterization of this click reaction by SEC analysis turned out to be much more difficult. We found that although the PDEAEMA side chain polymer was soluble in DMF, the brushes were not; a click reaction that was attempted in DMF resulted in the formation of an insoluble polymer immediately. While we were able to characterize the PDEAEMA side chain polymer by SEC using THF as solvent, the brushes could not be eluted out from the SEC system with THF as eluent – no high molecular weight brush peak was observed. Therefore, the reaction was characterized by ^1H NMR spectroscopy analysis; using the peak of $-\text{COOCH}_2$ (4.10-3.90 ppm) in the polymers as internal reference, the conversion of the reaction was calculated from the integral decrease of the peak at 4.62 ppm from alkyne end group ($\text{CH}\equiv\text{CCH}_2-$) of PDEAEMA (Figure S4). By using this conversion and the feed ratio of azide moieties to side chains, we calculated the grafting density

of PDEAEMA brushes to be 82.0 %, which is slightly higher than that of MBB-B (75.0%). This is reasonable because PDEAEMA was shorter than PDEAEMA-*b*-PTEGMA and thus the steric hindrance in the “click” grafting to synthesis would be smaller, allowing for a higher grafting density. The MBB-H brushes were purified by passing of the reaction mixture through an alumina/silica gel column to remove the copper catalyst and fractionation in a mixture of THF and hexanes to remove the unreacted side chain polymer, which was confirmed by ¹H NMR analysis that showed the disappearance of the alkyne end group peak (Figure S4). The molecular characteristics of MBB-B and MBB-H are summarized in Table 1.

Dynamic Light Scattering (DLS) Study and Visual Inspection of Stimuli-Responsive Behavior of MBB-B and -H in Aqueous Buffer Solution. To study the responsive property of MBB-B and the hypothesized stabilization effect of the PTEGMA outer block for the collapsed PDEAEMA side chains at high pH under ambient conditions, a 1.0 mg/g solution of MBB-B in a 10 mM phosphate buffer with a pH of 5.00 was made and the pH was gradually increased at room temperature by adding 0.1 M NaOH. For comparison, a 0.5 mg/g solution of MBB-H in 10 mM phosphate buffer was also prepared at pH = 5.00. The MBB-B solution remained transparent without any change in appearance when the pH was gradually increased from 5.00 to 10.00; Figure 2i and ii show the photos of the clear solutions at pH = 5.00 and 9.54 at ambient temperature (~ 21 °C). The 0.5 mg/g aqueous solution of MBB-H was clear when the pH was lower than 7.3 at room temperature (Figure 2v shows a photo at pH = 5.00). However, when the pH was raised to > 7.3, a precipitate was formed immediately in the solution (Figure 2vi shows a photo at pH = 8.00). Evidently, the outer PTEGMA blocks can stabilize the collapsed PDEAEMA blocks at higher pH.

Figure 3A shows the apparent average hydrodynamic size (D_h) of 1.0 mg/g MBB-B in a 10 mM phosphate buffer solution as a function of pH in the process of increasing pH (black solid

squares) under ambient conditions. In the entire pH range from 5.00 to 10.00, a single size distribution was observed; the hydrodynamic size distribution curves for pH = 6.00 and 8.50 are shown in Figure 3B as examples. Moreover, at pH = 6.00, the size distributions of MBB-B at concentrations of 0.5 and 1.0 mg/g essentially overlapped and the D_h values were virtually the same (Figure S6A), indicating that the brushes were molecularly dissolved in acidic buffers.

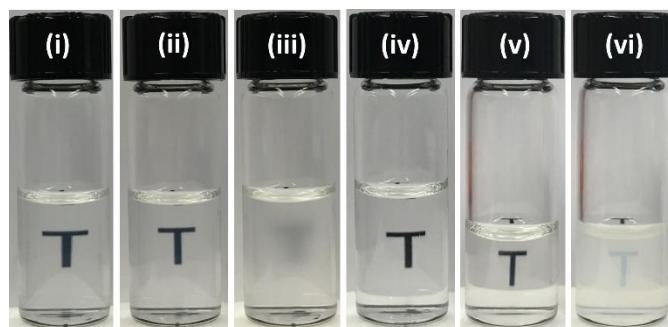


Figure 2. Optical photos of 1.0 mg/g solutions of MBB-B in 10 mM aqueous phosphate buffers at (i) pH = 5.00 and 21 °C, (ii) pH = 9.54 and 21 °C, and (iii) pH = 9.54 and 65 °C, of (iv) a 0.2 mg/g solution of MBB-B in phosphate buffer at pH = 9.54 and 65 °C, and of 0.5 mg/g solutions of MBB-H in phosphate buffer at (v) pH = 5.00 and (vi) pH = 8.00 under ambient conditions.

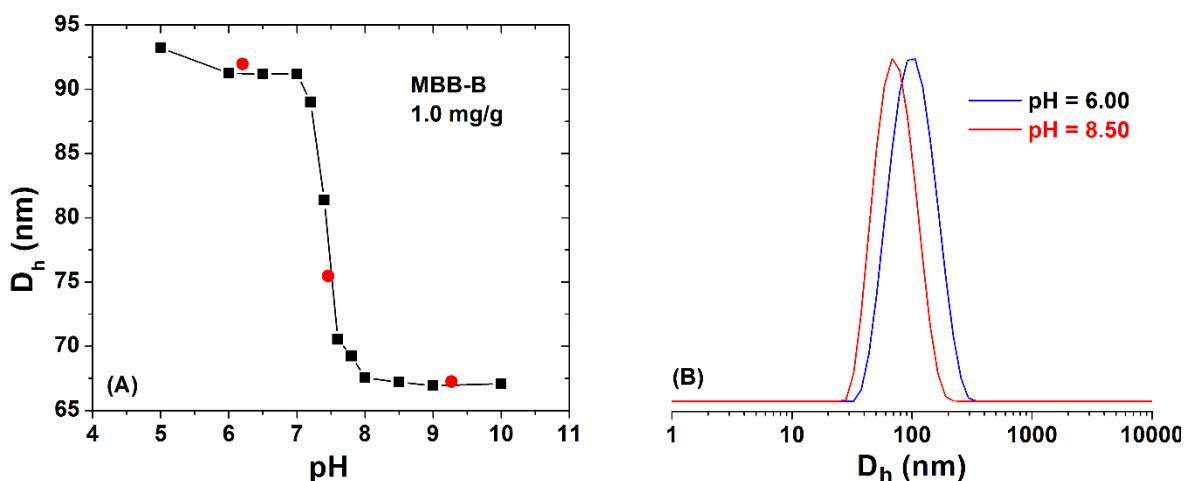


Figure 3. (A) Apparent average hydrodynamic size (D_h) of MBB-B in 10 mM phosphate buffer at a concentration of 1.0 mg/g at 25 °C as function of pH, adjusted using 0.1 M NaOH and 0.1 M HCl, in the process of increasing pH (black squares) and decreasing pH (red circles). (B) Hydrodynamic size distributions of 1.0 mg/g MBB-B in 10 mM buffer at pH = 6.00 and 8.50 at 25 °C.

As shown in Figure 3A, when the pH was < 7.2 , the sizes of MBB-B at different pH values were similar, decreasing only very slightly from 93.2 nm at pH = 5.00 to 91.2 nm at pH = 7.00. Upon further increasing pH, a sharp decrease in D_h was observed in a rather narrow pH range, from 89.0 nm at pH = 7.20 to 70.5 nm at pH = 7.60. When the pH was > 8.00 , the apparent hydrodynamic size leveled off at 67 nm. Thus, from pH = 5.00 to 10.00, the D_h decreased by 26 nm (or by 28%). A similar size transition was observed for the concentration of 0.5 mg/g (Figure S7). These observations agreed well with the reported $pK_a = 7.4$ of PDEAEMA homopolymer. At lower pH values, the PDEAEMA blocks in the brush molecules were protonated, and the MBB-B brushes took on an extended conformation, exhibiting larger hydrodynamic sizes. Upon increasing the solution pH above pK_a , deprotonation occurred and the PDEAEMA blocks became insoluble, causing the brushes to collapse into a more compact structure. The unimolecular extended-to-compact conformation transition was supported by the large reduction in D_h and single size distributions at pH $> pK_a$ as well as the observation that the size distributions of MBB-B at concentrations of 0.5 and 1.0 mg/g essentially superimposed each other for pH = 8.50 (Figure S6B). The pH-induced size changes were reversible. We lowered the pH value of the 1.0 mg/g MBB solution to 9.27, 7.46, and 6.20; a single size distribution was observed for each pH value, and the hydrodynamic sizes fell on the curve (red solid circles in Figure 3A).

We also studied the pH-responsive behavior of PDEAEMA homopolymer brushes MBB-H in aqueous buffers at a concentration of 0.2 mg/g (Figure 4) by DLS. At pH of 5.06, the average size was 76.3 nm with a single symmetric size distribution. Upon gradually increasing the pH to 7.0, the D_h decreased slightly to 74.0 nm, followed by a larger reduction to 68.7 nm at pH = 7.10 and then 67.1 nm at 7.25. Further raising the pH to 7.35 resulted in an increase in D_h and a much broader distribution with a large shoulder as shown in Figure 4B, indicating intermolecular

aggregation even at a concentration as low as 0.2 mg/g. This stands in stark contrast to the behavior of MBB-B, whose size leveled off at $\text{pH} > 8.0$ with a single narrow size distribution. Thus, we can conclude that the PTEGMA outer blocks in MBB-B provided a stabilization effect to the collapsed PDEAEMA inner blocks at ambient conditions.

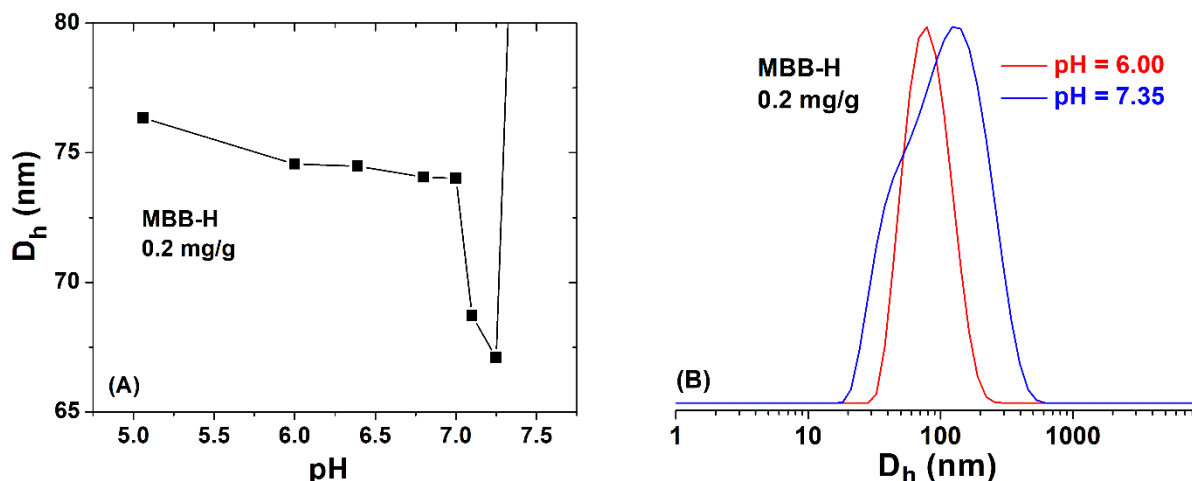


Figure 4. Apparent average hydrodynamic size (D_h) of MBB-H in 10 mM phosphate buffer at a concentration of 0.2 mg/g as function of pH. (B) Hydrodynamic size distribution curves of 0.2 mg/g MBB-B in 10 mM phosphate buffer at $\text{pH} = 6.00$ and 7.35 under ambient conditions.

As mentioned earlier, PTEGMA is a thermo-responsive water-soluble polymer with a LCST of $58\text{ }^\circ\text{C}$.^{44,45} As expected, when heated across the LCST of PTEGMA, the 1.0 mg/g solution of MBB-B with a pH of 9.54 turned cloudy as shown in Figure 2iii for the sample at $65\text{ }^\circ\text{C}$, indicating the aggregation of the MBB-B brush molecules due to the collapse of PTEGMA blocks. The thermoresponsive behavior of 1.0 mg/g MBB-B in 10 mM phosphate buffer at $\text{pH} = 8.50$ was studied by DLS. Figure 5 shows the plots of scattering intensity and D_h versus temperature from 20 to $65\text{ }^\circ\text{C}$ in a heating process. At each selected temperature, the solution was equilibrated for 5 min prior to the measurements. Interestingly, the scattering intensity increased slightly and the size showed a steady decrease upon heating until $\sim 60\text{ }^\circ\text{C}$. The D_h decreased by $\sim 10\text{ nm}$ in this

temperature range, reaching 58 nm at 58 °C. This can be attributed to the solvent quality for PTEGMA decreasing gradually with increasing temperature but still remaining within the good solvent regime, which was also previously observed for other PEO-based thermoresponsive polymers.^{45,46} Note that aqueous solutions of PDEAEMA with a concentration of 2.0 mg and MBB-H with a concentration of 1.0 mg/g in 10 mM phosphate buffer at pH = 7.10 were found to become cloudy upon heating (Figure S8), a sign of LCST transitions, although both solutions stayed clear from 0 to 100 °C at pH = ~ 6.0 (pH = 6.13 for PDEAEMA and pH 6.00 for MBB-H). It could be possible that the collapsed PDEAEMA inner blocks in MBB-B brush molecules at pH = 8.50 undergo further shrinking with increasing temperature, contributing to the size decrease observed in Figure 5B. Above 60 °C, sharp changes in scattering intensity and D_h were observed. In fact, the solution turned cloudy. The decrease in scattering intensity might be due to the settling of aggregates during the equilibration. Note that when the brush concentration was 0.2 mg/g, the solution stayed clear at 65 °C (Figure 2iv) and DLS showed that the brushes remained unaggregated above the LCST (Figure S9) and the thermally induced size changes were reversible. This is consistent with our previous observation for thermoresponsive brushes in H₂O.^{24,26}

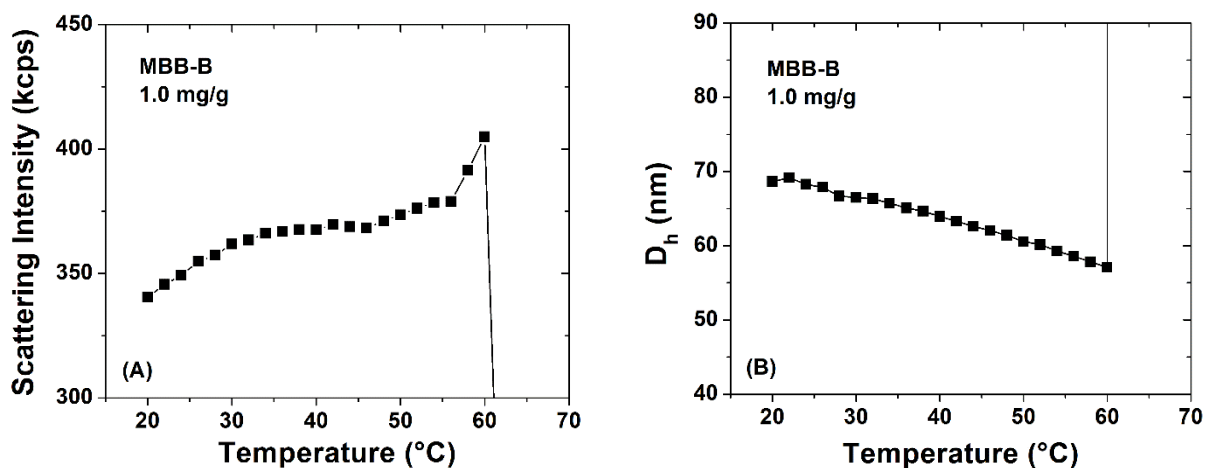


Figure 5. Plots of (A) scattering intensity and (B) D_h versus temperature for a 1.0 mg/g MBB-B solution in 10 mM phosphate buffer with pH of 8.50 from a DLS study in a heating process.

AFM Study of Responsive Behavior of MBB-B Molecular Brushes. The observed abrupt decrease in D_h of MBB-B in aqueous buffer with increasing pH across the pK_a of PDEAEMA suggests a transition of brush molecules from a more extended structure at lower pH to a more compact conformation at higher pH values, where the deprotonated PDEAEMA inner blocks collapsed and aggregated, forming a hydrophobic core that was supported in solution by the hydrophilic PTEGMA block at ambient conditions. To study the morphologies of MBB-B brush molecules under various conditions and to characterize their possible shape transitions, AFM was employed. Dilute aqueous solutions of MBB-B with concentrations from 0.05 mg/g to 0.1 mg/g in 2.5 mM phosphate buffer were prepared and spin cast onto PMMA-coated mica.

Figures 6 and S10 show AFM height images of MBB-B at pH = 5.00; as expected, the brush molecules were clearly in a cylindrical state, with an average contour length of 110.4 ± 13.8 nm and a typical height of ~ 6 nm. The brushes were taller than thermoresponsive binary heterografted molecular brushes on the same type of substrate that we observed before, which was about 1 nm,²⁶ likely due to the incorporation of counter-anions into the brushes at the low pH value as well as electrostatic repulsive forces present in the protonated tertiary amine groups, causing the side chains and backbone to adopt a more stretched conformation. When the pH of the solution was increased to 9.56 at room temperature, the MBB-B brushes collapse into much more condensed globular shape as shown in Figures 7 and S11 compared with cylindrical nano-objects in Figures 6 and S10. Some brush molecules appeared to be not fully collapsed into a spherical shape but exhibited a condensed C- or S-like shape. One possible factor that might contribute to this behavior is the relatively long PTEGMA outer block ($DP = 58$); the strong solvation of PTEGMA blocks in the collapsed state might make it difficult for brush molecules to reach a fully collapsed structure.

Cross-sectional analysis showed that the typical height of globular nano-objects was ~ 5.5 nm; the average size was 61.9 ± 9.2 nm.

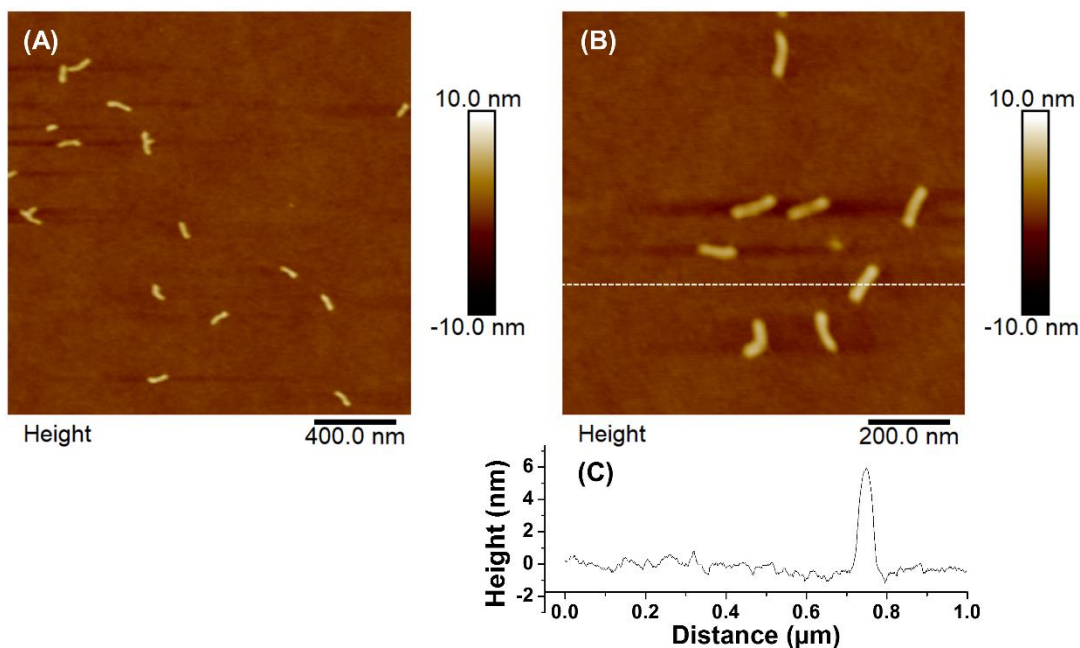


Figure 6. AFM height image (A) with sizes of 2×2 μm and (B) with sizes of 1×1 μm of MBB-B molecular brushes spin cast onto PMMA-coated mica at 3000 rpm from a 2.5 mM aqueous phosphate buffer solution with a polymer concentration of 0.05 mg/g at a pH of 5.00 and room temperature. (C) is the cross-sectional height profile along the dash line in image (B).

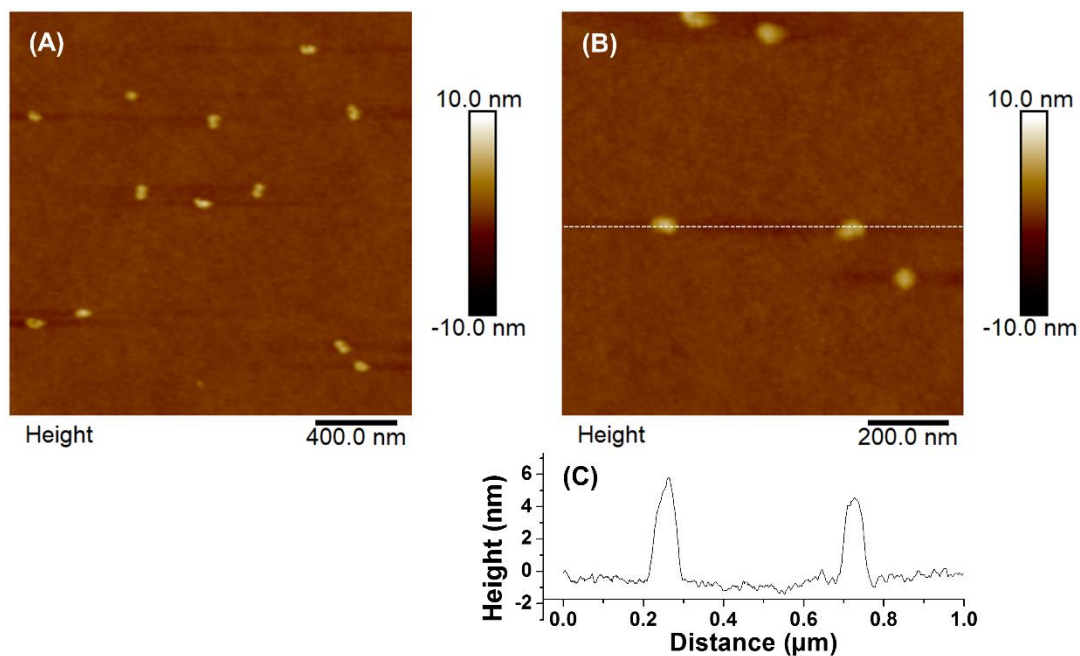


Figure 7. AFM height image (A) with sizes of 2×2 μm and (B) with sizes of 1×1 μm of MBB-B molecular brushes spin cast onto PMMA-coated mica at room temperature from a 2.5 mM

aqueous phosphate buffer solution at a pH of 9.56 with polymer concentration of 0.05 mg/g. (C) is the cross-sectional height profile along the dash line in image (B).

To study the thermally induced transition of MBB-B at $\text{pH} > \text{p}K_a$, we gradually increased the temperature of a 0.1 mg/g sample with a pH of 9.54 to 65 °C, which was above the LCST transition of PTEGMA, equilibrated it at the same temperature, and then spin cast on PMMA-coated mica for AFM imaging. As shown in Figures 8 and S12, the brush molecules remained as individually collapsed nano-objects but more condensed and spherical compared with the collapsed nano-objects in Figures 7 and S11 at the same pH but room temperature. This is consistent with the results by visual inspection and DLS analysis for a 0.2 mg/g solution of MBB-B in phosphate buffer (Figure 2iv and Figure S9). Analysis showed that the average size was 56.4 ± 7.5 nm and the typical height was ~ 7.5 nm, in contrast to 61.9 ± 9.2 nm and ~ 5.5 nm, respectively, for the brushes at room temperature. Evidently, the thermally induced LCST transition of PTEGMA outer blocks caused the globular MBB-B brushes to further collapse into a more spherical conformation in order to minimize the contact with surrounding water, as schematically illustrated in Scheme 2.

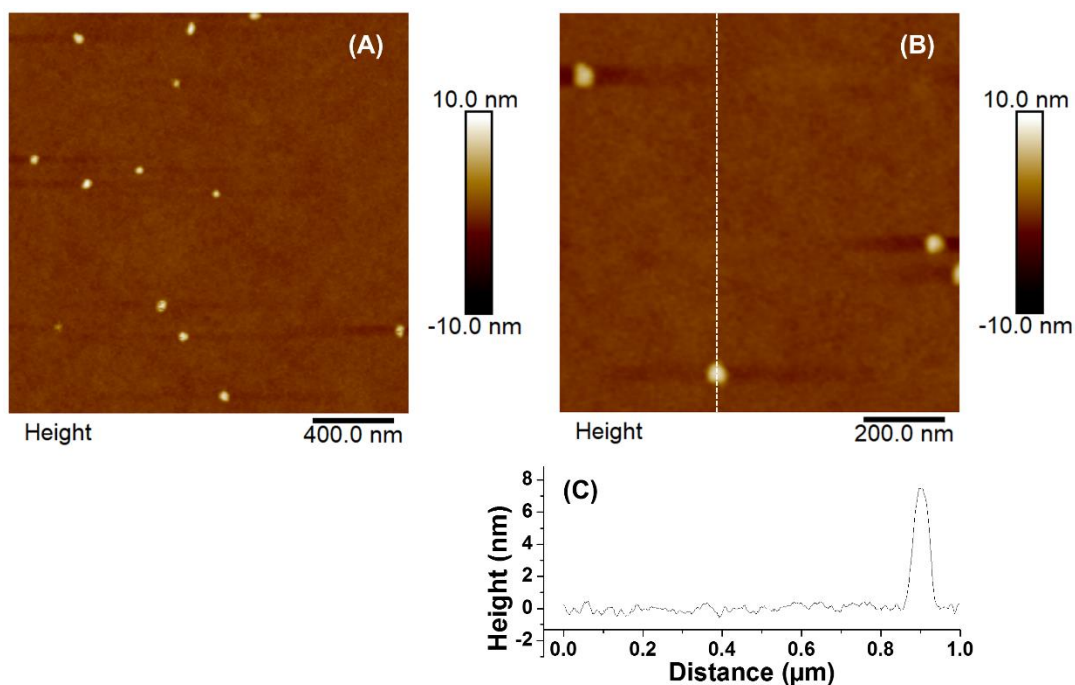
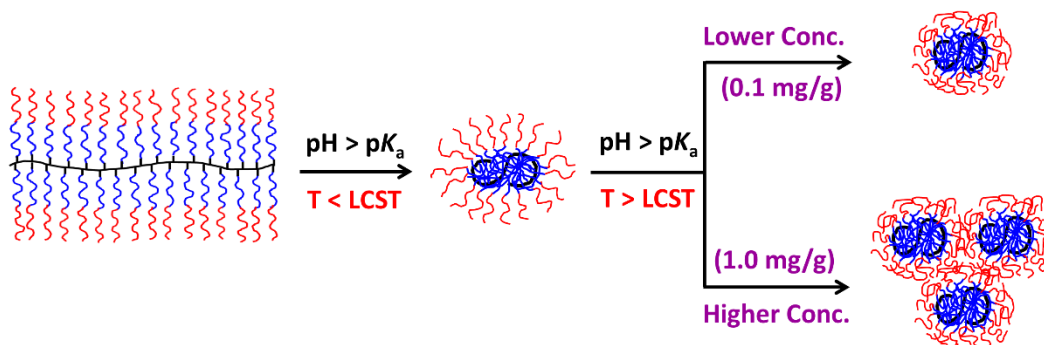


Figure 8. AFM height image (A) with sizes of $2 \times 2 \mu\text{m}$ and (B) with sizes of $1 \times 1 \mu\text{m}$ of MBB-B molecule brushes spin cast onto PMMA coated mica from a 0.1 mg/g solution of MBB-B in 2.5 mM phosphate buffer with a pH of 9.54 after being heated to 65 °C. (C) is the cross-sectional height profile along the dash line in image (B).

Scheme 2. Schematic Illustration of pH-Induced Cylinder-to-Globule Shape Transition and Temperature-Induced Further Condensation at Lower Concentration and Aggregation at Higher Concentration.



As shown in Figures 2iii and 5, at $\text{pH} > \text{p}K_a$ of PDEAEMA and a concentration of 1.0 mg/g, the MBB-B brush molecules underwent aggregation and the solution turned cloudy upon heating above the LCST of PTEGMA. To investigate the morphology of the aggregated brush molecules, a 1.0 mg/g sample with a pH of 9.57 was heated to 65 °C and it turned cloudy. The sample was then diluted quickly to 0.1 mg/g at 65 °C and spin cast onto PMMA-coated mica. AFM study revealed the presence of large tight clusters (Figures 9 and S13) as well as spherical nano-objects, which confirmed the intermolecular aggregation of brushes (Scheme 2).

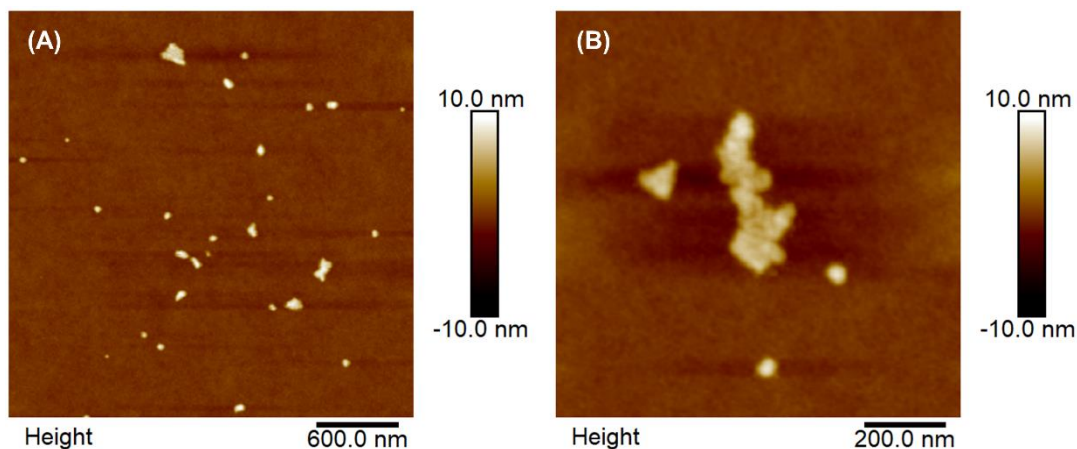


Figure 9. AFM height image (A) with sizes of $3 \times 3 \mu\text{m}$ and (B) with sizes of $1 \times 1 \mu\text{m}$ of MBB-B molecular brushes spin cast onto PMMA-coated mica from a 0.1 mg/g aqueous solution of MBB-B that was diluted at 65 °C from a 1.0 mg/g aqueous solution of MBB-B in 2.5 mM buffer with a pH of 9.57. The 1.0 mg/g solution was heated to 65 °C before the dilution.

Conclusions

In summary, we synthesized linear homografted molecular brushes containing dually pH- and thermo-responsive diblock copolymer side chains by a click “grafting to” method and demonstrated that the introduction of a second block to the end of the inner pH-responsive block in the grafted side chains effectively stabilized the collapsed brushes when the inner blocks became insoluble in water. DLS study showed that the D_h of MBB-B exhibited a sharp drop in a narrow pH range when the pH was raised across the pK_a of PDEAEMA and leveled off at higher pH values. AFM revealed a cylindrical morphology of the brushes at acidic pH and a cylinder-to-globule transition with increasing pH. Moreover, the solution state of the brushes can be further controlled by the temperature and the brush concentration. At lower concentrations such as 0.1 mg/g, the brushes remained as individual nano-objects in solution and became more spherical at temperatures above the LCST of PTEGMA, while at higher concentrations (e.g., 1.0 mg/g) aggregation occurred and the solution turned cloudy. In contrast, the brushes with only pH-responsive side chains aggregated and precipitated out when the solution pH was around pK_a and

above. It is our belief that the method reported in this work to achieve worm-to-stabilized globule transition and control the solution state of collapsed brushes could open up new opportunities for potential applications of stimuli-responsive shape-changing molecular brushes such as tailoring of the morphology of nanomaterials synthesized by using molecular brushes as template.

Electronic Supplementary Information Available: Characterization data for backbone and side chain polymers as well as molecular brushes; additional DLS data and AFM images. See DOI: 10.1039/xxxxxxx.

Acknowledgements: This work was supported by NSF through DMR-1607076.

ORCID

Bin Zhao: 0000-0001-5505-9390

References:

1. J. Y. Yuan, A. H. E Müller, K. Matyjaszewski and S. S. Sheiko, Molecular Brushes, In *Polymer Science: A Comprehensive Reference, 10 Volume Set*. Vol. 6, Elsevier, 2012, pp. 199-264. DOI: 10.1016/B978-0-444-53349-4.00164-3.
2. S. S. Sheiko, B. S. Sumerlin and K. Matyjaszewski, *Prog. Polym. Sci.*, 2008, **33**, 759-785.
3. M. F. Zhang and A. H. E Müller, *J. Polym. Sci. Part A: Polym. Chem.*, 2005, **43**, 3461-3481.
4. Y. Xia, B. D. Olsen, J. A. Kornfield and R. H. Grubbs, *J. Am. Chem. Soc.*, 2009, **131**, 18525-18532.
5. X. Banquy, J. Burdyńska, D. W. Lee, K. Matyjaszewski and J. Israelachvili, *J. Am. Chem. Soc.*, 2014, **136**, 6199–6202.
6. W. F. Daniel, J. Burdynska, M. Vatankhah-Varnoosfaderani, K. Matyjaszewski, J. Paturej, M. Rubinstein, A. V. Dobrynin and S.S. Sheiko, *Nat. Mater.*, 2016, **15**, 183–189.

7. J. A. Johnson, Y. Y. Lu, A. O. Burts, Y. Xia, A. C. Durrell, D. A. Tirrell and R. H. Grubbs, *Macromolecules*, 2010, **43**, 10326–10335.
8. Y. Gai, D.-P. Song, B. M. Yavitt and J. J. Watkins, *Macromolecules*, 2017, **50**, 1503-1511.
9. J. Liu, A. O. Burts, Y. Li, A. V. Zhukhovitskiy, M. F. Ottaviani, N. J. Turro and J. A. Johnson, *J. Am. Chem. Soc.*, 2012, **134**, 16337– 16344.
10. K. Matyjaszewski, S. Qin, J. R. Boyce, D. Shirvanyants and S. S. Sheiko, *Macromolecules*, 2003, **36**, 1843-1849.
11. C. Cheng, K. Qi, E. Khoshdel and K. L. Wooley, *J. Am. Chem. Soc.*, 2006, **128**, 6808–6809.
12. M. B. Runge and N. B. Bowden, *J. Am. Chem. Soc.*, 2007, **129**, 10551-10560.
13. H. Lu, J. Wang, Y. Lin and J. J. Cheng, *J. Am. Chem. Soc.*, 2009, **131**, 13582– 13583.
14. Z. Li, J. Ma, C. Cheng, K. Zhang and K. L. Wooley, *Macromolecules*, 2010, **43**, 1182– 1184.
15. J. Bolton and J. Rzyayev, *ACS Macro Lett.*, 2012, **1**, 15-18.
16. R. Fenyves, M. Schmutz, I. J. Horner, F. V. Bright and J. Rzyayev, *J. Am. Chem. Soc.*, 2014, **136**, 7762– 7770.
17. H. Luo, M. Szymusiak, E. A. Garcia, L. L. Lock, H. Cui, Y. Liu and M. Herrera-Alonso, *Macromolecules*, 2017, **50**, 2201– 2206.
18. Y. Shi, W. Zhu and Y. M. Chen, *Macromolecules*, 2013, **46**, 2391–2398.
19. D. Han, X. Tong and Y. Zhao, *Macromolecules*, 2011, **44**, 5531-5536.
20. H. Tang, Y. Li, S. H. Lahasky, S. S. Sheiko and D. Zhang, *Macromolecules*, 2011, **44**, 1491– 1499.
21. P. Zhao, Y. Yan, X. Feng, L. Liu, C. Wang and Y. Chen, *Polymer*, 2012, **53**, 1992-2000.
22. H. F. Gao and K. Matyjaszewski, *J. Am. Chem. Soc.*, 2007, **129**, 6633-6639.

23. R. K. Iha, K. L. Wooley, A. M. Nyström, D. J. Burke, M. J. Kade and C. J. Hawker, *Chem. Rev.*, 2009, **109**, 5260-5685.
24. D. M. Henn, W. X. Fu, S. Mei, C. Y. Li and B. Zhao, *Macromolecules*, 2017, **50**, 1645– 1656.
25. D. M. Henn, C. M. Lau, C. Y. Li and B. Zhao, *Polym. Chem.*, 2017, **8**, 2702– 2712.
26. D. M. Henn, J. A. Holmes, E. W. Kent and B. Zhao, *J. Phys. Chem. B*, 2018, **122**, 7015–7025.
27. H.-I Lee, J. Pietrasik, S. S. Sheiko and K. Matyjaszewski, *Prog. Polym. Sci.*, 2010, **35**, 24-44.
28. H.-I. Lee, J. Pietrasik and K. Matyjaszewski, *Macromolecules*, 2006, **39**, 3914– 3920.
29. S.-i. Yamamoto, J. Pietrasik and K. Matyjaszewski, *Macromolecules*, 2007, **40**, 9348– 9353.
30. C. Li, N. Gunari, K. Fischer, A. Janshoff and M. Schmidt, *Angew. Chem. Int. Ed.*, 2004, **43**, 1101-1104.
31. H.-I Lee, J. R. Boyce, A. Nese, S. S. Sheiko and K. Matyjaszewski, *Polymer*, 2008, **49**, 5490– 5496.
32. Y. Xu, S. Bolisetty, M. Drechsler, B. Fang, J. Yuan, M. Ballauff and A. H. E. Müller, *Polymer*, 2008, **49**, 3957–3964.
33. N. Gunari, Y. Cong, B. Zhang, K. Fischer, A. Janshoff and M. Schmidt, *Macromol. Rapid Commun.*, 2008, **29**, 821– 825.
34. Y. Xu, S. Bolisetty, M. Ballauff and A. H. E. Müller, *J. Am. Chem. Soc.*, 2009, **131**, 1640– 1641.
35. C. Li, Z. Ge, J. Fang and S. Liu, *Macromolecules*, 2009, **42**, 2916–2924.
36. X. Li, H. ShamsiJazeyi, S. L. Pesek, A. Agrawal, B. Hammouda and R. Verduzco, *Soft Matter*, 2014, **10**, 2008-2015.
37. S. S. Sheiko, S. A. Prokhorova, K. L. Beers, K. Matyjaszewski, I. I. Potemkin, A. R. Khokhlov and M. Möller, *Macromolecules*, 2001, **34**, 8354-8360.

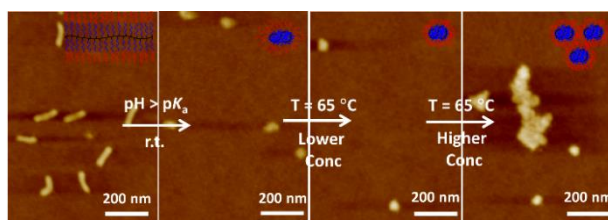
38. F. Sun, S. S. Sheiko, M. Moeller, K. Beers and K. Matyjaszewski, *J. Phys. Chem. A*, 2004, **108**, 9682–9686.
39. M. O. Gallyamov, B. Tartsch, A. R. Khokhlov, S. S. Sheiko, H. G. Boerner, K. Matyjaszewski and M. Möller, *Chem. - Eur. J.*, 2004, **10**, 4599–4605.
40. J. Yao, Y. Chen, J. Zhang, C. Bunyard and C. Tang, *Macromol. Rapid Commun.*, 2013, **34**, 645-651.
41. E. Kutnyanszky, M. A. Hempenius and G. J. Vancso, *Polym. Chem.*, 2014, **5**, 771-783.
42. D. M. Henn, R. A. E. Wright, J. W. Woodcock, B. Hu and B. Zhao, *Langmuir*, 2014, **30**, 2541–2550.
43. K. J. Zhou, Y. G. Wang, X. N. Huang, K. Luby-Phelps, B. D. Sumer and J. M. Gao, *Angew. Chem., Int. Ed.*, 2011, **50**, 6109–6114.
44. F. J. Hua, X. G. Jiang, D. J. Li and B. Zhao, *J. Polym. Sci. Part A: Polym. Chem.*, 2006, **44**, 2454-2467.
45. N. X. Jin, J. W. Woodcock, C. M. Xue, T. G. O’Lenick, X. G. Jiang, S. Jin, M. D. Dadmun and B. Zhao, *Macromolecules*, 2011, **44**, 3556-3566.
46. N. X. Jin, H. Zhang, S. Jin, M. D. Dadmun and B. Zhao, *J. Phys. Chem. B*, 2012, **116**, 3125-3137.
47. Z. F. Bai and T. P. Lodge, *J. Phys. Chem. B*, 2009, **113**, 14151–14157.
48. J. M. Horton, Z. F. Bai, T. P. Lodge and B. Zhao, *Langmuir*, 2011, **27**, 2019–2027.

Table of Contents Entry

Title: *Shape-Changing Linear Molecular Bottlebrushes with Dually pH- and Thermo-Responsive Diblock Copolymer Side Chains*

Authors: *Ethan W. Kent, Daniel M. Henn, and Bin Zhao*

Table of Contents Graphic and Abstract:



The collapse of inner pH-responsive blocks drives cylindrical-to-globular shape transition while outer thermoresponsive blocks provide additional control of solution state.